relation based on free and forced convection

$$[Nu_{MC}]^n = [Nu_{NC}]^n + [Nu_{FC}]^n, \quad n = 3. \tag{12}$$

4. CONCLUSION

Numerical results have been reported for two-dimensional, steady free, forced and mixed convection from a flush-mounted, isoflux heat source on one vertical wall of the channel the walls of which are otherwise adiabatic. In the free convection regime, the flow may separate from the unheated wall at high Grashof numbers, and if the channel is long, it may reattach at a distance far away from the heat source. The recirculating flow, however, disappears as the Reynolds number increases. The strength and extent of the convective cell depend strongly on Grashof and Reynolds numbers and show the possibility of flow entrainment at the exit end if the channel is short.

The heat transfer rate is also a strong function of Grashof and Reynolds number. Depending on the Grashof number, it may be either lower or higher than the vertical plate solutions. However, in the forced convection regime, it is always lower than the flat plate results. The mixed convection Nusselt numbers can be easily predicted by a composite relation based on the free and forced convection values (equation (14)). The present problem, however, does not fall into the category for which free and mixed convection Nusselt numbers can be predicted from the forced convection correlations as proposed by Ortega and Moffat for discretely heated channels [2]. Also, these results neither support the theory that the Nusselt numbers for the present problem are always lower than the vertical plate solutions in the free convection regime, nor do they agree with the observation of several authors that the discrete heating always results in higher heat transfer rates. Finally, we expect that numerical results reported here will provide a basis for better understanding of the effects of shrouding and wall protuberances, as well as the influence of both the upstream and downstream adiabatic sections.

REFERENCES

1. A. D. Kraus and A. Bar-Cohen, *Thermal Analysis and Control of Electronic Equipment*, pp. 303–320. Hemisphere, New York (1983).
2. R. J. Moffat and A. Ortega, Direct air cooling of electronic components. In *Advances in Thermal Modelling of Electronic Components and Systems* (Edited by A. Bar-Cohen and A. D. Kraus), pp. 129–262. Hemisphere, New York (1988).
3. Y. Jaluria, Natural convection cooling of electronic equipment. In *Natural Convection: Fundamentals and Applications* (Edited by S. Kakac *et al.*), pp. 961–986. Hemisphere, New York (1985).
4. T. L. Ravine and D. E. Richards, Natural convection heat transfer from a discrete thermal source on a channel wall, *J. Heat Transfer* **110**, 1004–1007 (1988).
5. T. L. Ravine and D. E. Richards, Natural convection heat transfer from a discrete thermal source on a vertical surface, *J. Heat Transfer* **110**, 1007–1009 (1988).
6. A. Ortega and R. J. Moffat, Heat transfer from an array of simulated electronic components: experimental results for free convection with and without a shrouding wall. In *Heat Transfer in Electronic Equipment—1985* (Edited by S. Oktay and R. J. Moffat), ASME-HTD Vol. 48, pp. 5–15 (1985).
7. S. Ramanathan and R. Kumar, Correlations for natural convection between heated vertical plates, *Proc. ASME Winter Annual Meeting* (1988); also in *J. Heat Transfer* (in press).
8. F. C. Lai, V. Prasad and F. A. Kulacki, Aiding and opposing mixed convection in a vertical porous layer with a finite wall heat source, *Int. J. Heat Mass Transfer* **31**, 1049–1061 (1988).
9. G. C. Vliet, Natural convection local heat transfer on constant heat-flux inclined surfaces, *J. Heat Transfer* **91**, 511–516 (1969).
10. R. A. Wirtz and R. J. Stutzman, Experiments on free convection between vertical plates with symmetric heating, *J. Heat Transfer* **104**, 501–507 (1982).
11. W. M. Kays and M. E. Crawford, *Convective Heat and Mass Transfer*, 2nd Edn. McGraw-Hill, New York (1980).
12. H. S. Heaton, W. C. Reynolds and W. M. Kays, Heat transfer in annular passages. Simultaneous development of velocity and temperature fields in laminar flow, *Int. J. Heat Mass Transfer* **7**, 763–781 (1964).

Int. J. Heat Mass Transfer. Vol. 34, No. 2, pp. 578–582, 1991
Printed in Great Britain

0017-9310/91 $3.00 + 0.00

Film condensation on an upward facing plate with free edges

ADRIAN BEJAN
Department of Mechanical Engineering and Materials Science, Duke University, Durham, NC 27706, U.S.A.

(*Received* 12 *December* 1989 *and in final form* 20 *April* 1990)

INTRODUCTION

THE PURPOSE of this note is to report several laminar film condensation results that apply to a basic geometric configuration—the plane horizontal surface that faces upward. Reviews of the laminar film condensation field [1–3] have shown that solutions have been developed for a wide variety of wall shapes and orientations, e.g. vertical and inclined plates, horizontal and inclined cylinders, a sphere, and several types of rotating surfaces. It has been recognized also that the phenomenon of condensation on a horizontal flat surface can behave in more than one way, depending on whether the surface faces upward or downward. The case of the downward facing plate was treated by Gerstmann and Griffith [4], who showed that the condensate film develops a bumpy surface (cf. the Taylor instability) from which droplets leave the film intermittently.

The upward facing plate is discussed by Rohsenow [1], but only under the assumption that the plate serves as the bottom surface for a vessel with adiabatic vertical walls. In that case, the lateral walls prevent the horizontal motion of the condensate, and the time-dependent growth of the film thickness is described by the one-dimensional (vertical) conduction solution associated with the classical Stefan problem.

NOMENCLATURE

B	dimensionless parameter, equations (26), (27) and (29)
c_P	specific heat at constant pressure
D	diameter of horizontal disc, Fig. 1
f	function, equation (3)
g	gravitational acceleration
h_f	enthalpy of saturated liquid
h_{fg}	latent heat of condensation, or vaporization
h'_{fg}	modified latent heat of condensation, or vaporization
h_g	enthalpy of saturated vapor
$\bar{h}_D$	disc-averaged heat transfer coefficient, equation (19)
$\bar{h}_H$	H-averaged heat transfer coefficient, equation (21)
$\bar{h}_L$	L-averaged heat transfer coefficient, equation (15)
H	height of vertical surface, Fig. 2
$\tilde{H}$	enthalpy flow rate, equation (8)
k	thermal conductivity
L	width of horizontal strip, Fig. 1
$\dot{m}(r)$	condensation flow rate on disc of radius r, equation (16)
$\overline{Nu}_D$	disc Nusselt number, equation (19)
$\overline{Nu}_H$	vertical surface Nusselt number, equation (21)
$\overline{Nu}_L$	horizontal strip Nusselt number, equation (15)
P	pressure in the liquid, equation (3)
P_{vap}	pressure in the vapor, equation (4)
q'	total heat transfer rate into the strip, per unit length of strip, equation (13)
r	radial position
$\hat{r}$	dimensionless radial position, equation (18)
T_{sat}	saturation temperature, and temperature of liquid–vapor interface
T_w	temperature of solid surface
u	horizontal liquid velocity, pointing toward the edge
x	horizontal position across the strip, Fig. 1
y	vertical position above the horizontal surface, Fig. 1
z	vertical position down (along) the vertical surface, Fig. 2.

Greek symbols

$\Gamma(x)$	condensation flow rate collected on the horizontal strip, equation (7)
δ	thickness of horizontal film
$\tilde{\delta}$	dimensionless film thickness on the strip, equation (11)
δ	dimensionless film thickness on the disc, equation (18)
$\Delta(z)$	condensation flow rate on the vertical surface, equation (23)
λ	thickness of vertical film, equation (24)
μ	viscosity
ξ	dimensionless horizontal position, equation (11)
Π_H	dimensionless group, equation (22)
ρ	density.

Subscripts

l	liquid
v	vapor.

A third horizontal plate configuration is the upward facing plate with free edges. This geometry forms the subject of this note. In this configuration, the condensate flows away from the central region of the plate, and spills over the edge. The film reaches a steady state, as the rate at which vapor condenses on the surface of the film is balanced by the liquid flow rate integrated along the edge. These two fundamental characteristics—the tangential flow of liquid, and the steady-state thickness of the film—distinguish this configuration from the bottom-of-vessel case treated in the handbook [1].

THE HORIZONTAL STRIP

Consider first the two-dimensional geometry of Fig. 1, in which the long dimension of a strip of width L is oriented in the direction perpendicular to the plane of the figure. The cold plate (at temperature T_w) faces an atmosphere of stagnant saturated vapor (which is at temperature T_{sat}). Of interest is the total rate of condensation on the length L, or the heat transfer rate into the plate, per unit length in the direction normal to the figure.

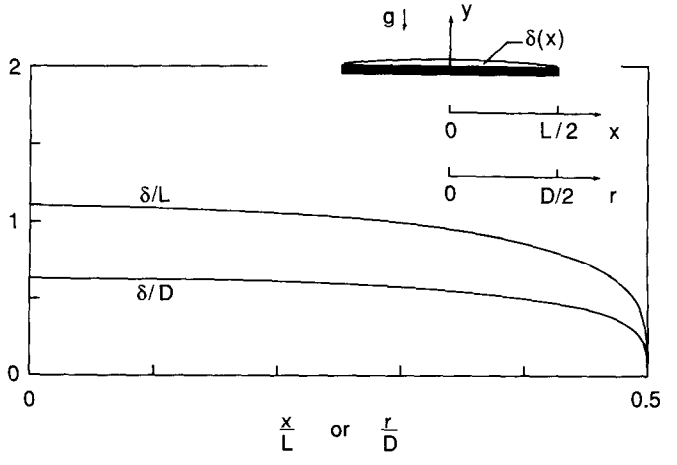

FIG. 1. The film condensate on a horizontal strip of width L, or a disc of diameter D.

The following analysis is of the same simplified type (i.e. Nusselt type) as that found in most textbooks for the vertical plate problem [5], therefore we can review only the key steps and then examine the results. The liquid film is treated as a boundary layer with negligible inertia effect, therefore the momentum equations are

$$0 = -\frac{\partial P}{\partial x} + \mu_l \frac{\partial^2 u}{\partial y^2} \tag{1}$$

$$0 = -\frac{\partial P}{\partial y} - \rho_l g. \tag{2}$$

Integrated, equation (2) reads

$$P(x,y) = -\rho_l g y + f(x) \tag{3}$$

for which $f(x)$ is determined by matching the liquid pressure to that of the vapor at their mutual interface ($y = \delta$). The pressure distribution in the vapor is hydrostatic

$$P_{vap}(y) = -\rho_v g y + \text{constant} \tag{4}$$

therefore, by writing $P(x,\delta) = P_{vap}(\delta)$ we determine $f(x)$ and, more importantly

$$\frac{\partial P}{\partial x} = (\rho_l - \rho_v) g \frac{d\delta}{dx}. \tag{5}$$

Together, equations (1) and (5) allow us to determine the horizontal velocity profile

$$u(x,y) = \frac{g}{\mu_l}(\rho_l - \rho_v)\delta^2 \frac{d\delta}{dx}\left[\frac{1}{2}\left(\frac{y}{\delta}\right)^2 - \frac{y}{\delta}\right] \tag{6}$$

which is based on assuming no slip at the solid wall, and zero shear at the liquid–vapor interface. The local liquid flow rate, per unit length normal to the plane of Fig. 1, is

$$\Gamma(x) = \rho_l \int_0^\delta u \, dy = -\frac{\rho_l g}{3\mu_l}(\rho_l - \rho_v)\delta^3 \frac{d\delta}{dx}. \tag{7}$$

Under the assumption that the temperature distribution across the film is linear, the enthalpy flow rate carried by the condensate film through the plane x = constant is

$$\tilde{H}(x) = [h_f - \tfrac{3}{8} c_{p,l}(T_{sat} - T_w)]\Gamma(x). \tag{8}$$

The first law statement for the control volume of size $(\delta) \times (dx)$ reduces to

$$h'_{fg}\, d\Gamma = \frac{k_l}{\delta}(T_{sat} - T_w)\, dx \tag{9}$$

in which $h'_{fg} = h_{fg} + \frac{3}{8} c_{p,l}(T_{sat} - T_w)$. Combined with the expression for $\Gamma(x)$ derived earlier, equation (9) becomes an equation for the film thickness function

$$-\tilde{\delta}\frac{d}{d\xi}\left(\tilde{\delta}^3 \frac{d\tilde{\delta}}{d\xi}\right) = 3 \tag{10}$$

where the dimensionless variables are

$$\xi = \frac{x}{L}, \quad \tilde{\delta} = \delta\left[\frac{h'_{fg}\rho_l(\rho_l - \rho_v)g}{k_l(T_{sat} - T_w)\mu_l L^2}\right]^{1/5}. \tag{11}$$

The variables can be separated in equation (10) by relying on the auxiliary function $A = d\tilde{\delta}^4/d\xi$. Integrating once, and using the midplane condition that $\tilde{\delta} = \tilde{\delta}_0$ (unknown) at $\xi = 0$, where, due to symmetry, $A = 0$, we obtain

$$2^{1/2}\frac{d\xi}{d\tilde{\delta}} = -\frac{\tilde{\delta}^3}{(\tilde{\delta}_0^3 - \tilde{\delta}^3)^{1/2}}. \tag{12}$$

The final step is the integration of this equation, by properly choosing the midplane thickness $\tilde{\delta}_0$ so that the $\tilde{\delta}(\xi)$ solution satisfies the edge condition $\tilde{\delta}(1/2) = 0$. Worth noting is that the condition of zero film thickness at the edge of the plane does not mean that the liquid flow rate vanishes at the edge. On the contrary, one can easily verify that the flow rate reaches its largest (finite) value at the edge. My reason for using the zero-thickness condition at the edge is that the equivalent of this condition was used in the boundary layer treatment of single-phase natural convection on a cold upward facing plate, where it was shown that the resulting solution agrees well with empirical results [6].

The integration of equation (12) was performed numerically by marching in 7000 equal steps of $\tilde{\delta}$, from $\tilde{\delta} = \tilde{\delta}_0$ to 0. This means that the corresponding steps in ξ have a much higher density near the edge than in the central section of the plate. The film thickness solution $\tilde{\delta}(\xi)$ is presented as δ/L in Fig. 1, in which the correct choice for the midplane thickness, $\tilde{\delta}_0 = 1.105$, is accurate within 0.5%.

The total heat transfer rate into the L-wide plate is

$$q' = 2\int_0^{L/2} k_l \frac{T_{sat} - T_w}{\delta}\, dx$$

$$= 2k_l L(T_{sat} - T_w)\left[\frac{h'_{fg}\rho_l(\rho_l - \rho_v)g}{k_l(T_{sat} - T_w)\mu_l L^2}\right]^{1/5} \int_0^{1/2} \frac{d\xi}{\tilde{\delta}}. \tag{13}$$

The numerical value of the integral shown on the right-hand side turns out to be 0.539. The total rate of condensate is proportional to the heat transfer rate absorbed by the plate

$$2\Gamma(L) = \frac{q'}{h'_{fg}}. \tag{14}$$

These conclusions can be summarized in dimensionless form by defining a Nusselt number based on the L-averaged heat transfer coefficient $\bar{h}_L$

$$\overline{Nu}_L = \frac{\bar{h}_L L}{k_l} = 1.079\left[\frac{h'_{fg}\rho_l(\rho_l - \rho_v)gL^3}{k_l(T_{sat} - T_w)\mu_l}\right]^{1/5}. \tag{15}$$

The main difference between this solution and Nusselt's corresponding $\overline{Nu}_l$ formula for laminar film condensation on a vertical plate is the exponent of the dimensionless group formed on the right-hand side. In the vertical plate case, that exponent is $\frac{1}{4}$ (see equation (21) later in this note).

THE HORIZONTAL DISC

A completely analogous analysis can be made for the laminar film of condensate on a circular plate of diameter D. In what follows we review only the key results, beginning with the radial liquid flow rate through the cylindrical cut of radius r

$$\dot{m}(r) = -\frac{2\pi}{3}\frac{\rho_l g}{\mu_l}(\rho_l - \rho_v) r \delta^3 \frac{d\delta}{dr}. \tag{16}$$

The first-law analysis of the ring-shaped control volume of height δ, radius r, and radial thickness dr leads to a differential equation for the film thickness

$$\hat{r}\hat{\delta}^4 \frac{d^2\hat{\delta}}{d\hat{r}^2} + 3\hat{r}\hat{\delta}^3\left(\frac{d\hat{\delta}}{d\hat{r}}\right)^2 + \hat{\delta}^4 \frac{d\hat{\delta}}{d\hat{r}} + 3\hat{r} = 0 \tag{17}$$

with the following definitions:

$$\hat{r} = \frac{r}{D/2}, \quad \hat{\delta} = \delta\left[\frac{h'_{fg}\rho_l(\rho_l - \rho_v)g}{k_l(T_{sat} - T_w)\mu_l(D/2)^2}\right]^{1/5}. \tag{18}$$

Equation (17) was integrated numerically subject to the conditions $d\hat{\delta}/d\hat{r} = 0$ at $\hat{r} = 0$, and $\hat{\delta} = 0$ at $\hat{r} = 1$. The $\hat{r}$ domain was divided into 7000 steps of equal size, and the calculation started from $\hat{r} = 0$, where a value for the film thickness ($\hat{\delta}_0$) had to be assumed. The proper value turned out to be $\hat{\delta}_0 = 1.268$.

The resulting solution for the film thickness is shown in Fig. 1. This solution is presented in terms of δ/D and r/D, to invite a comparison with the film that would build on a horizontal strip of the same width as D. On the disc, the film is noticeably thinner because the condensate can run in all the directions away from the central region.

The Nusselt number based on the disc-averaged heat transfer coefficient $\bar{h}_D$ is

$$\overline{Nu}_D = \frac{\bar{h}_D D}{k_l} = 1.368\left[\frac{h'_{fg}\rho_l(\rho_l-\rho_v)gD^3}{k_l(T_{sat}-T_w)\mu_l}\right]^{1/5}. \quad (19)$$

This formula is similar to the $\overline{Nu}_L$ formula obtained for the horizontal strip, equation (15). The larger numerical factor on the right-hand side of equation (19) is a consequence of the fact that on the disc the film is thinner than on a horizontal strip of the same width as D.

The total condensation rate generated by the upward facing disc, $\dot{m}(D/2)$, equation (16), is proportional to the total heat transfer rate absorbed by the disc, cf. equation (19)

$$\dot{m}\left(\frac{D}{2}\right) = \frac{q}{h'_{fg}} = \frac{\pi}{4}D^2\frac{\bar{h}_D}{h'_{fg}}(T_{sat}-T_w). \quad (20)$$

THE VERTICAL SLAB WITH HORIZONTAL TOP SURFACE

The upward facing surfaces treated until now may serve as 'roofs' for three-dimensional objects surrounded by saturated vapor (Fig. 2). It is important to note that the condensation on the horizontal top surface affects the total rate of condensation on the body in *two* ways. It contributes *directly* through the flow rate estimated based on equation (14) or equation (20), and *indirectly* by thickening the film that coats the vertical lateral surface. The indirect effect forms the subject of this section.

The classical result for laminar film condensation on a vertical surface of height H is [3–5]

$$\overline{Nu}_H = \frac{\bar{h}_H H}{k_l} = 0.943\Pi_H^{1/4} \quad (21)$$

in which the dimensionless group Π_H is based on H as the length scale

$$\Pi_H = \frac{h'_{fg}\rho_l(\rho_l-\rho_v)H^3}{k_l(T_{sat}-T_w)\mu_l}. \quad (22)$$

This result applies also to a curved vertical surface (e.g. Fig. 2, right), provided the thickness of the vertical film is small relative to H.

The analytical derivation of equation (21) has historically been based on the assumption that the thickness of the vertical film $\lambda(z)$ is zero at the top edge of the vertical surface. In the present case, the starting thickness of the vertical film is finite, $\lambda(0) = \lambda_0$, because of the condensate flow generated by the top surface. Omitting most of the analysis, we record only the formulas for the vertical flow rate down the side wall

$$\Delta(z) = \frac{g\rho_l}{3\mu_l}(\rho_l-\rho_v)\lambda^3(z) \quad (23)$$

the thickness of the vertical film

$$\lambda(z) = \left[\lambda_0^4 + \frac{k_l(T_{sat}-T_w)\mu_l}{h'_{fg}\rho_l(\rho_l-\rho_v)g}4z\right]^{1/4} \quad (24)$$

and, finally, the H-averaged heat transfer coefficient

$$\frac{\bar{h}_H H}{k_l} = 0.943\Pi_H^{1/4}[(1+B)^{3/4}-B^{3/4}] \quad (25)$$

where the group B is shorthand for

$$B = \frac{1}{4}\left(\frac{\lambda_0}{H}\right)^4\Pi_H. \quad (26)$$

By comparing equation (25) with equation (21), we see that the quantity in square brackets in equation (25) accounts for the film-thickening effect of the liquid collected by the top surface. The B parameter can be calculated by writing that the horizontal flow that spills over the edge, $\Gamma(L)$, is the same as the starting flow rate of the vertical boundary layer. This last equation pinpoints the value of λ_0 and, in the end, the value of the B parameter needed in the heat transfer coefficient formula (25):

$$B = 0.475\left(\frac{L}{H}\right)^{4/5}\Pi_H^{-1/15}. \quad (27)$$

The factor in the square brackets in equation (25) is less than 1, regardless of the value of B. In conclusion, the indirect effect of the condensate formed on the top surface is to partially inhibit the film condensation process that occurs on the vertical lateral surface.

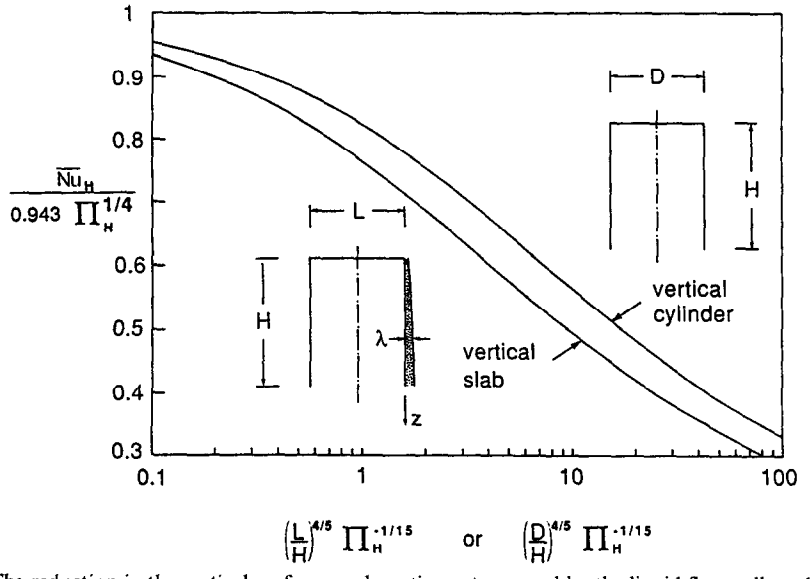

FIG. 2. The reduction in the vertical-surface condensation rate, caused by the liquid flow collected on the top surface.

THE VERTICAL CYLINDER WITH HORIZONTAL TOP SURFACE

Equation (25) describes also the H-averaged heat transfer coefficient on the vertical surface of the cylinder shown on the right-hand side of Fig. 2. What changes in the present case is only the expression for parameter B, which follows from the condition of mass continuity over the circular edge of the top surface

$$\frac{1}{\pi D}\dot{m}\left(\frac{D}{2}\right) = \Delta(0). \tag{28}$$

After using equations (19), (20), (23) and (24), we obtain

$$B = 0.259\left(\frac{D}{H}\right)^{4/5}\Pi_{\bar{H}}^{1/15}. \tag{29}$$

This B expression is similar to the one for the vertical face of a slab with a flat top, equation (27). Again, the effect of the flow rate of condensate produced by the disc-shaped top surface is to decrease the condensation rate that would have been produced by the vertical surface in the absence of the disc. This effect is presented graphically in Fig. 2, the abscissa of which reveals a new dimensionless group that can be written alternatively as $(D/H)\Pi_{\bar{H}}^{1/12}$

REFERENCES

1. W. M. Rohsenow, Film condensation. In *Handbook of Heat Transfer* (Edited by W. M. Rohsenow and J. P. Hartnett), Section 12A. McGraw-Hill, New York (1973).
2. H. Merte, Jr., Condensation heat transfer, *Adv. Heat Transfer* **9**, 181–272 (1973).
3. J. H. Lienhard, *A Heat Transfer Textbook* (2nd Edn), Section 9.5. Prentice-Hall, Englewood Cliffs, New Jersey (1987).
4. J. Gerstmann and P. Griffith, Laminar film condensation on the underside of horizontal and inclined surfaces, *Int. J. Heat Mass Transfer* **10**, 567–580 (1967).
5. W. Nusselt, Die Oberflächenkondensation der Wasserdampfes, *Z. Ver. Dt. Ing.* **60**, 541–569 (1916).
6. S. Kimura, A. Bejan and I. Pop, Natural convection near a cold plate facing upward in a porous medium, *J. Heat Transfer* **107**, 819–825 (1985).

Int. J. Heat Mass Transfer. Vol. 34, No. 2, pp. 582–587, 1991
Printed in Great Britain

0017–9310/91 $3.00 + 0.00

Mixed forced and natural convection from two-dimensional or axisymmetric bodies of arbitrary contour

M. R. CAMERON,† D. R. JENG‡ and K. J. DEWITT§

† Polymer Institute, The University of Toledo, Toledo, OH 43606, U.S.A.
‡ Department of Mechanical Engineering, The University of Toledo, Toledo, OH 43606, U.S.A.
§ Department of Chemical Engineering, The University of Toledo, Toledo, OH 43606, U.S.A.

(*Received* 17 *July* 1989 *and in final form* 3 *April* 1990)

1. INTRODUCTION

MIXED convection problems involving laminar boundary layers have been treated in a variety of ways. Most solutions found thus far have been valid only over a limited range of the buoyancy parameters, i.e. they represent situations perturbed from either the pure forced or natural convection cases. Two sets of solutions must be obtained in order to have valid results for the entire range. Some of the early studies on mixed convection have dealt only with similarity solutions. For example, Sparrow *et al.* [1] pointed out that for an isothermal wedge, a similarity solution only existed for a wedge angle of 120°. Mixed convection for the vertical and the horizontal plate have also been discussed by Schneider [2], Lloyd and Sparrow [3], Sparrow and Minkowycz [4], Chen *et al.* [5], Ramachandran *et al.* [6] and Raju *et al.* [7]. For the horizontal plate, the momentum equation in the direction normal to the plate must be accounted for in order to obtain meaningful results. The integral of the temperature function adds complexity to the numerical solution when this momentum equation is included. Solution techniques have been mostly local similarity or local non-similarity in nature. Wedge flow was analyzed by Gunness and Gebhart [8]. They perturbed the Falkner–Skan equation for a situation including the buoyancy effects in directions both along and normal to the surface. Their perturbation quantities, however, were related to the buoyancy parameter which limited the results to relatively small effects. Mixed convective flow for inclined plate and sphere geometries were investigated by Mucoglu and Chen [9, 10]. Both local non-similarity [11, 12] and Keller and Cebeci's [13] finite-difference algorithm were used to solve the laminar boundary layer equations which represented the system perturbed from forced and/or free convection. A good reference which summarizes the literature for mixed convection is the new text of Gebhart *et al.* [14].

In the present study, an analysis is made for mixed convection in laminar boundary layer flow over two-dimensional or axisymmetric isothermal surfaces with arbitrary contour. The laminar boundary layer equations for mixed convection are transformed and formulated in such a way that they are valid over the entire range of concern, from pure forced convection to pure natural convection. The Merk–Chao series [15, 16] for two parameters is developed in this paper and is applied to obtain the solution for mixed convection. By introducing this two-parameter Merk–Chao series into the transformed boundary layer equations, there results a set of ordinary differential equations with two parameters which implicitly absorb the geometry and orientation of the surface. Therefore, by assigning numerical values to these parameters, this set of equations can be solved so that the results for the flow field and the heat transfer can be expressed in terms of universal functions.

The purpose of this study was (i) to obtain a set of transformations which would allow the boundary layer equations to be solved for the entire mixed convection range, (ii) to adapt the Merk–Chao expansion to these mixed convection equations, and (iii) to formulate modified definitions for the friction factor group and the Nusselt number group which are finite for the full mixed convection range. Section 2 of this paper illustrates the development of the transforms plus it presents the expansion used. A comparison of the solutions to the resultant equations with previous investigations is covered in Section 3. Finally, the modified definitions for